BIO Web of Conferences **163**, 04002 (2025) https://doi.org/10.1051/bioconf/202516304002
ICBBB 2025

Quantitative evaluation of equation-based model in hypokalemic periodic paralysis condition with bistability

Wanchai Buntha[1] and *Nipon* Theera-Umpon[1]

[1]Biomedical Engineering Institute, Chiang Mai University, Thailand

Abstract. Hypokalemia in periodic paralysis (HypoPP) is usually not a straightforward hypokalemic condition. It is mainly characterized by the intercellular shift of potassium between compartments inside human body, not by depletion solely. Several experiments at the cellular level demonstrated the separation of resting membrane potential including the paradoxical depolarization possibly causing clinical manifestation. We analyzed the structural model focusing on the intracellular potassium pool and connected cellular electrophysiology information to the macroscale. Increment of extracellular potassium cannot be simply expected after potassium supplementation for hypokalemic correction which is different from general pharmacokinetics. Searching the bistable solutions from the existing bifurcation in a bounded parameter subset was the newly-introduced strategy for testing the possibility of pushing the solution to one another stable point as the representative of potassium falling or paradoxical hypokalemia instead of adding parameters or terms in the traditional way. Moreover, the continuous trajectories from the model combined with the difference between input and output and the proposed utilization from parameter mapping to alleviate the sudden falling of the solution were demonstrated. The results also supported the pre-existing hypothesis that NaK+-ATPase activation was responsible for this phenomenon.

1. Introduction

Potassium is the crucial electrolyte in the human body and is distributed in the cells and extracellular fluid. If the potassium level is within the normal range (approximately 3.5 to 5.0 mmol/L), they will function properly. However, the deviation from its range, like hypokalemia (lower than normal), can possibly lead to loss of function of cells and organs and if it sufficiently deviates, it may contribute to life-threatening complications such as respiratory muscle paralysis, cardiac arrhythmia, etc. [1,2]. Hypokalemia can be divided into 2 groups which are true reduction of total potassium and transcellular potassium shift from the extracellular to the intracellular compartment without loss. In some situations, both of them can occur together [3]. Hypokalemic periodic paralysis is a complicated medical condition consisting of hypokalemia and episodic muscle weakness. Even if it is rare but possibly lethal from severely low potassium level so the potassium administration is emergency management and it must be managed in time to reverse the pathologic process

[4,5]. The dynamic change of potassium level from the beginning until recovery is complicated. Unusual phenomena such as paradoxical hypokalemia (the level of potassium is lower after starting the treatment) and rebound hyperkalemia (the level of potassium is greater than the upper normal limit) were reported [6]. It is classified into 2 types that are nonfamilial and familial type [4]. Nonfamilial hypoPP is commonly caused by thyrotoxicosis (TPP). About one-third of patients with TPP had KCNJ12, KCNJ18 mutations causing impairment of Kir function which led to higher susceptibility of hypokalemia when combined with NaK+- ATPase pump activation [4,7]. Gene mutations of familial type are mostly characterized by CACNA1S or SCN4A mutation leading to the aberrant gating pore current and indirect reduction of Kir conductance by uncertain mechanisms [4,8,9]. Some previous models involving potassium dynamics were found to have some limitations in this context. For example, Stadt et.al.[10] and Ursino et.al.[11] demonstrated the potassium shift by the gradient but did not link to the membrane potential properties, van Milet.al.[12] and Delmoe et.al.[13] demonstrated bistability of membrane potential from paradoxical depolarization when lowering the potassium concentration in the experimental setup but did not link to the whole-body scale. Therefore, the study attempted to fill the gap in the model hierarchy. Although there was the variability of sites of mutation when delving down to channels [9], for quantitative consequences, this work initially selected the necessary components in the equations which were expected to yield the behavior differently, but they should not be complicated. The parameter identification was implemented and TPP would be the prototype for study. This work has been inspired by the assumption that the total potassium is not depleted in real practice. Therefore, some constraints were applied to test if it was promising to be explainable in cellular and whole-body level simultaneously.

2. Model setup

2.1 Main Components

For simplification, the compartments were divided into 2 parts which are intracellular and extracellular part as shown in Fig 1. Since muscle cells are responsible for the largest potassium reservoir [14], the selected potassium-related channels in muscle cells for modeling can be assumed to adequately capture the overall potassium dynamics.

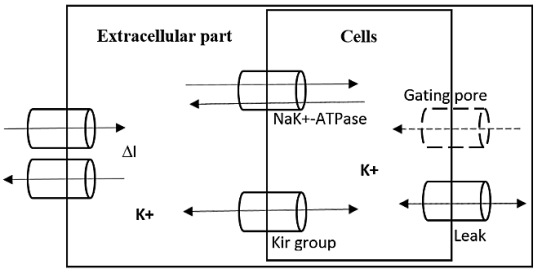

Fig 1. Schematic representation of the divided compartments and the involving protein channels

The governing equations are as follows.

$$I = V_{out}\frac{d[K_{out}]}{dt} = I_{nak}+I_{kir}+I_L+I_{gp}+\Delta I \quad , \quad V_{in}\frac{d[K_{in}]}{dt} = -(I_{nak}+I_{kir}+I_L+I_{gp}) \tag{1}$$

$$I_{nak} = -c_{Jnak}.Jnak.\left(\frac{[K_{out}]}{[K_{out}]+k_k}\right)^2 \ , \ Jnak = Jnak_0.\left(\frac{[Na_{in}]}{[Na_{in}]+k_{na}}\right)^3 \tag{2}$$

$$I_{kir} = c_{Jkir}.J_{kir}.\left([K_{out}]^{nofK}\right).(V_m\text{-}E_K).\left(\frac{1}{1+e^{\frac{V_m\text{-}V_{0.5}}{k}}}\right) \ , \ E_K = \frac{RT}{F} ln\left(\frac{[K_{out}]}{[K_{in}]}\right) \quad (3)$$

$$I_L = c_{JL}.J_L.(V_m\text{-}V_{reverse}) \quad (4)$$

$$I_{gp} = J_{gp}.e^{-b_{factor}(V_m\text{-}V_{reverse\_gp})} \ , \ V_{reverse\_gp} \approx 0 \quad (5)$$

Added Constraints : From the evidence in [15], the membrane potential had a negative relationship to the inhibition or reduction of Kir conductance, so we simply assumed the positive relationship with intracellular K+ by considering the cells with some value of capacitance.

$$C\frac{dV_m}{dt} = FV_{in}\frac{d[K_{in}]}{dt} \text{ or } C(V_m\text{-}V_{m,0}) = FV_{in}([K_{in}]\text{-}[K_{in,0}]) \quad (6)$$

$$TotalK = V_{in}[K_{in}] + V_{out}[K_{out}] \quad (7)$$

Where V_{in} , V_{out} are extracellular and intracellular volume, $[K_{out}]$,$[K_{in}]$ are extracellular and intracellular K+ concentration, ΔI is net input-output rate of K+, V_m is membrane potential (voltage).

2.2 General numerical method

Firstly, 'Fmincon' in MATLAB with interior point algorithm was used for fitting to find some unknown parameters. Next, equilibrium points were calculated by dividing the interval with random guess together with 'Vpasolve' iteratively until no solution was detected in the subinterval. Then dynamic trajectories from ODEs were demonstrated by using 'ODE23s' with 'maxstep' adjustment and 'interp1' (linear interpolation) to obtain the output for each specific time point.

2.3 Parameter Identification or Re-identification

In the parameter identification process, we firstly obtained the values of parameters that were relatively consistent among different literatures and considered them as fixed parameters. 5 remaining parameters (*nofK*, c, J_{kir} , C and $V_{reverse}$) were identified properly with different methods later as described in table 1.

Table 1. The values of each parameter and a brief method of acquisition

Parameters	Estimated values	Units	Reference(s) or methods
k_k	1	mmol	[12], [14]
k	9	mV	[16]
$V_{0.5}$	-80	mV	[12] (The value was close to resting potential.)
$c=\frac{J_{kir}}{J_L}$	1.2	-	[17] , Used the equations above and set $[K_{out}]\approx 4$ and estimated by ratio of currents.
$[K_{in,0}]$	150	mmol/L	[18]
$Jnak_0$	100.8	mmol/min	[14]
$[Na_{in}]$	15	mmol/L	[19]
k_{na}	7	mmol	[12]
V_{out}	≈0.2*BW	L	[20]
$TotalK$	≈50*BW	mmol	[21]

nofK	1.22	-	[22], Re-identified with the ratio the maximum outward current at $[K_{out}] = 4$ and 2 which is 2.
$V_{m,0}$	-93.35	mV	[23]
J_{kir}	3.15	mmol/(min.mV)	Fit with [23]
C	104	C/mV	Fit with [23]
$V_{reverse}$	-73.3	mV	Fit with [23]

(Note that BW = body weight, V_{in} was calculated by equation (7) at $[K_{out}] = 4$, *nofK* was chosen to be re-identified because of inconsistency between [22] and [24].)

3. Results

3.1 Voltage-current relationship in the experimental condition and no-loss condition (with constraint)

$[K_{out}]$was set in the experimental container, $TotalK$ could not be determined. Fig 2. (left) shows the consistency of characteristics with preexisting works [12,13,16] even though there were some differences of terms or parameter values. If we put the constraints by assuming the linear relationship of $[K_{in}]$ and V_m and the mass conservation of $TotalK$, the shape of current-$[K_{in}]$ are not much different from the experimental condition as shown in Fig 2. (right). (Note that both were set in normal condition, stable solution is where *I* crosses x-axis.)

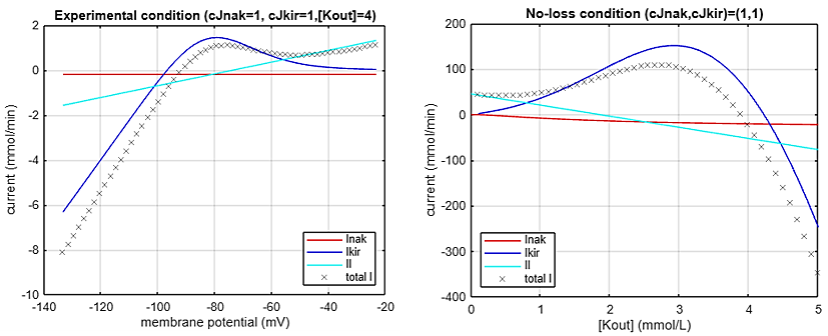

Fig 2. The current values from each channel in the given model in both experimental condition and no-loss condition

3.2 Identification of stable solution(s) in no-loss condition (with constraint)

To imitate the pathology of hypoPP, coefficients c_{Jnak} , c_{Jkir} , c_{JL} , J_{gp} were needed to change within some reasonable ranges. Firstly, we used TPP as the prototype for study leading to $c_{JL} = 1$ $J_{gpcoeff} = 0$. The remaining (c_{Jnak} , c_{Jkir}) were set in the range of ([1-6], (0-1]) which were a representative of NaK+-activation and Kir inhibition respectively. Then each parameter pair from sampling was calculated to demonstrate the equilibrium points by equating $\frac{d[K_{out}]}{dt} = 0$. Due to 1D autonomous ODE, equilibrium points that followed $\frac{d^2[K_{out}]}{dt^2}^* < 0$ were selected as stable solutions (assumed that the probability of $\frac{d^2[K_{out}]}{dt^2}^* = 0$ was negligible). Bistability is defined by having 2 stable points. After plotting the stable solutions, it was noticeable that the changes of stable solution values with respect to the change of c_{Jkir} are relatively higher at $[K_{out}]$ = [2-3] mmol/L then at some (c_{Jnak} , c_{Jkir}) values, the solutions were separated as bistability especially when c_{Jnak} was

relatively high. This characteristic confirms the existence of 2 main resting potentials within given parameters which mainly followed the experimental condition (Fig 3.).

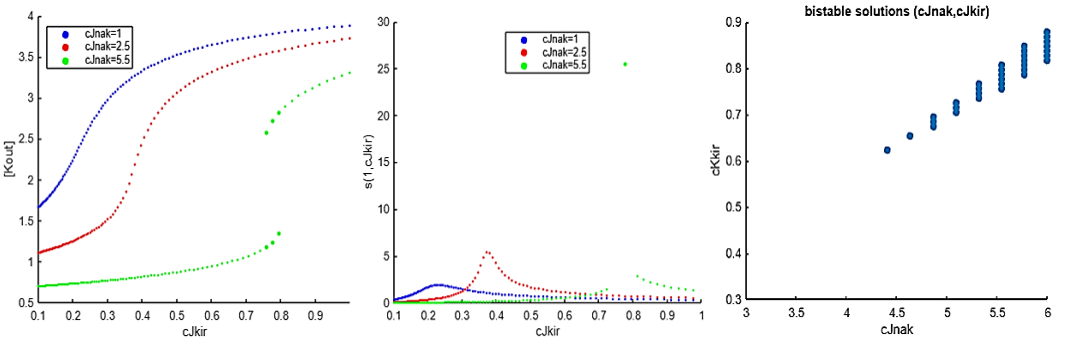

Fig 3. The example of plotted solutions with varying 1 parameter while fixing one another (left) with the derivative-based sensitivity that was calculated and plotted (middle). The big color dots represent the parameter pairs that have bistable solutions (right)

3.3 Potassium supplementation effect to the change of stable solutions

The typical pharmacokinetics expects that if the amount of the drug or substance increases in the body after administration via the oral or intravenous route, the measured quantity of them in the blood should increase but the significant number of TPP cases were found to have decreasing amount of [K_{out}] after K+ supplementation [25,26]. That led to the question. 'Is it possible to happen in the model with given parameters without adding more term to the equation?' Therefore, this part started introducing the potassium supplementation as an example of perturbation to the system and calculated the changes of stable solutions when *TotalK* increased. 3 patterns were found as shown in Fig 4. consisting of 1. monotonically increasing (left) 2. paradoxical falling of K+ starting with 2 stable solutions (middle) and 3. paradoxical falling of K+ starting with 1 stable solution (right).

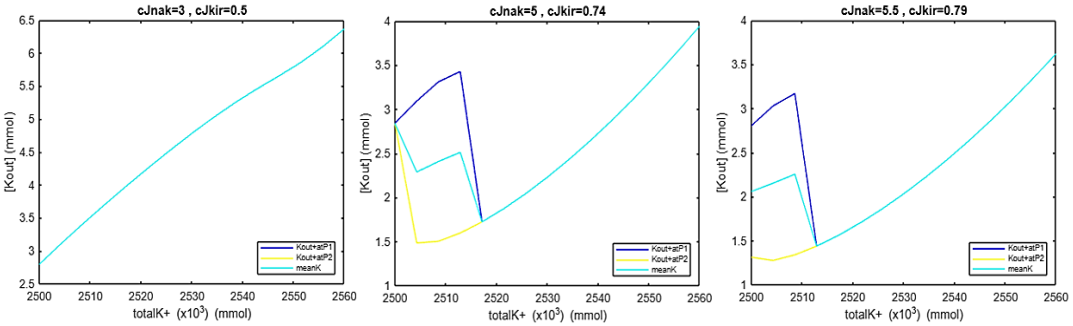

Fig 4. The plotted stable solutions from some (c_{Jnak} , c_{Jkir}) with different *TotalK* and after reaching at some *TotalK* value (there exists only 1 stable point for all cases.)

3.4 Dynamically numerical results

Running with ODEs with $\Delta I > 0$ gave the same patterns as the plot of stable points. For 2 initial [K_{out}], the real trajectory should lie between trajectories from both of them (this case was set as a mean) which could decrease the unrealistic sudden falling as shown in Fig 5. (right). However, for 1 initial [K_{out}], there is no way to alleviate the sudden falling of the solution itself. By comparing with Fig 4. (middle), it obviously demonstrates the shift of stable point to one another following the basin of attraction of the dynamical system.

Remark : 1. Sketching the stable solutions in 3.3 in parallel supported the underlying cause of trajectories' behavior. 2. this study set $\Delta I > 0$ to exclude the paradoxical falling of K+ from the excretion.

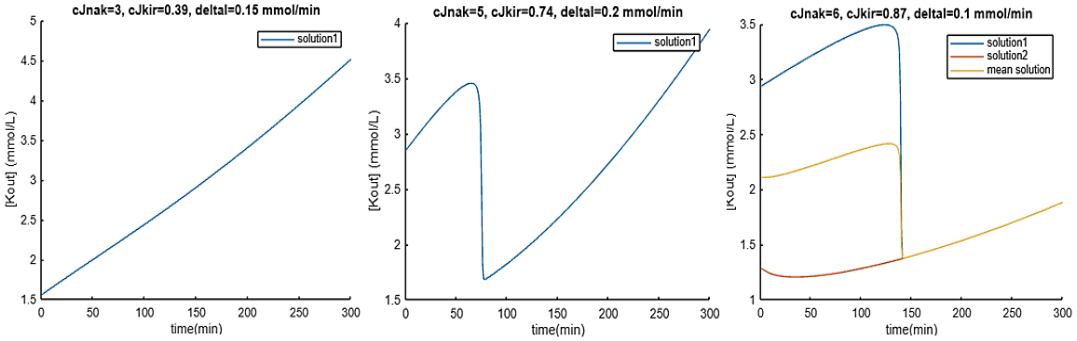

Fig 5. The plotted dynamical solutions from some (c_{Jnak} , c_{Jkir}) giving the 3 different patterns

3.5 Proposed parameter mapping method to alleviate the sharp falling of trajectories

In order to imitate and simulate the paradoxical K+ falling by relying on bistability but reduce the effect of sudden falling from the long distance between 2 stable points, the idea originated from the fact of heterogeneity of tissues, cell types, and protein channel properties. The different values of parameters as the representative of that property in each condition could possibly be responsible for giving the same output.

Step 1: Collect all stable solutions over a bounded parameter subset like (c_{Jnak} , c_{Jkir}) = ([1-6],[0.1-1]). Step 2: Use the mean if more than 1 solution are found because in reality, [K_{out}] must exist only 1 value. Step 3: Select the initial [K_{out}] of interest with a small deviated range like ±0.1 and arrange all corresponding parameter pairs. Step 4: Run ODEs for each of these with some value of ΔI, if min(output) < initial [K_{out}] then consider them in the 'drop' group, otherwise, 'not drop' group as seen in Fig 6. Step 5: Select some parameter pair in the yellow zone ('not drop' group) or the blue zone ('drop' group) but their values should be significantly different, add as the I_{new} component in equation (8) then run for numerical results as seen in Fig 7.

$$\frac{d[K_{out}]}{dt} = \beta I_{main} + (1-\beta) I_{new}\ ,\quad 0<\beta<1 \tag{8}$$

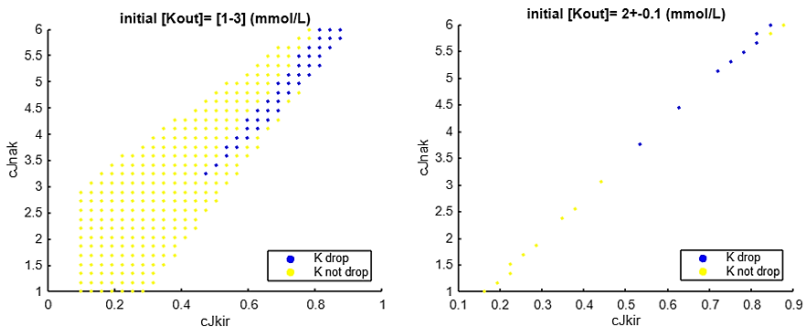

Fig 6. Parameter mapping with separation of 2 zones (left) and selection of initial [K_{out}] of interest (right)

By observing the values of parameter pairs in 2 zones, when comparing Fig 3. (right) to Fig 6. (left), not only parameter pairs that give initial bistable solutions but some nearby parameters lead to the paradoxical falling of trajectories of [K_{out}]. Moreover, the higher (c_{Jnak},c_{Jkir}) value within the parameter subset that gives the same or almost the same initial [K_{out}]. value has the greater probability of the paradoxical falling that occurs.

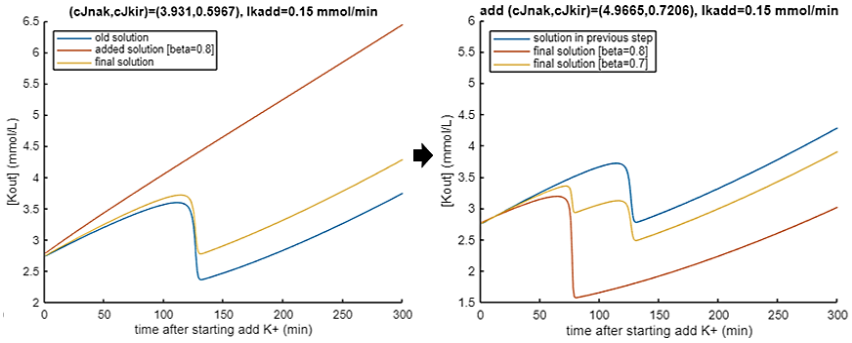

Fig 7. The examples trajectories after applying equation (8) to be more realistic

The right graph also shows the result from iterating the equation (8) by obtaining the final solution in the previous step, like the middle graph, that can reduce the overall sharpness of the falling curve and make it more realistic with a minimal change of the initial value. This is the example of method of fine-tuning trajectory without violating biological basis if we cannot avoid encountering with bistable solutions in the parameter subset. Moreover, parameter pairs from the blue color zone tend to take more time to reach a specific value due to the inward shift of K+ that could be used as the representative of poor or slow progressive response of K+ supplementation.

3.6 Familial hypoPP

This type has 1 additional exponential term as a representation of aberrant gating pore which is different from TPP case. There should exist a subset in the parameter space that exhibits an inverse response of membrane potential after reducing K+ concentration (paradoxical depolarization) [14,19]. Due to the variability of experimental data values from different settings, the simple direct searching method in parameter space was implemented starting from estimating suitable range of b_{factor} from Struyk et.al.[27] and we tested the increment of resting membrane potential from further inhibited cJ_{kir} from insulin infusion as seen in Fig 8. Due to the slightly higher values of stable V_m at the lower bound of J_{gp} compared with real values, we decreased $V_{reverse}$~10% (-80 mV) as an adjustment and the direction of change can still ensure the existence of solution(s) in the no-loss condition for macroscale. After testing with varying 100 values of cJ_{kir}, the parameter pairs in each value of fitting that could yield bistable solutions were depicted in both normal cJ_{nak} and activated NaK+-ATPase (cJ_{nak} was set to be 2) in Fig 9.

Moreover, the right column of Fig 9. also shows the proportion of parameter pairs (c_{Jnak} , c_{Jkir}) randomly selected from all possible parameter points giving bistable solutions as cJ_{nak} increased. Although the main characteristic of familial hypoPP is the exponential leak current, the increased probability of bistable solutions with increasing cJ_{nak} in the set of possible parameters has the same pattern as the TPP case.

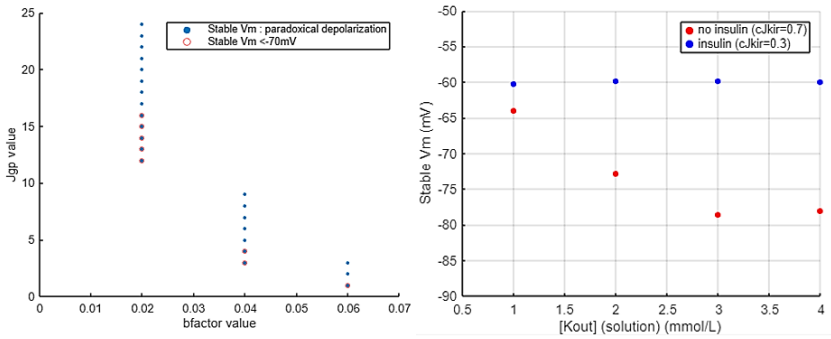

Fig 8. The illustration of the range of (J_{gp} ,b_{factor}) satisfying paradoxical depolarization and the example of bound determination or narrowing down the range to be more in line with the reality (i.e., no data reported that stable V_m at normal K+ in hypoPP condition exceeded 70 mV [23].

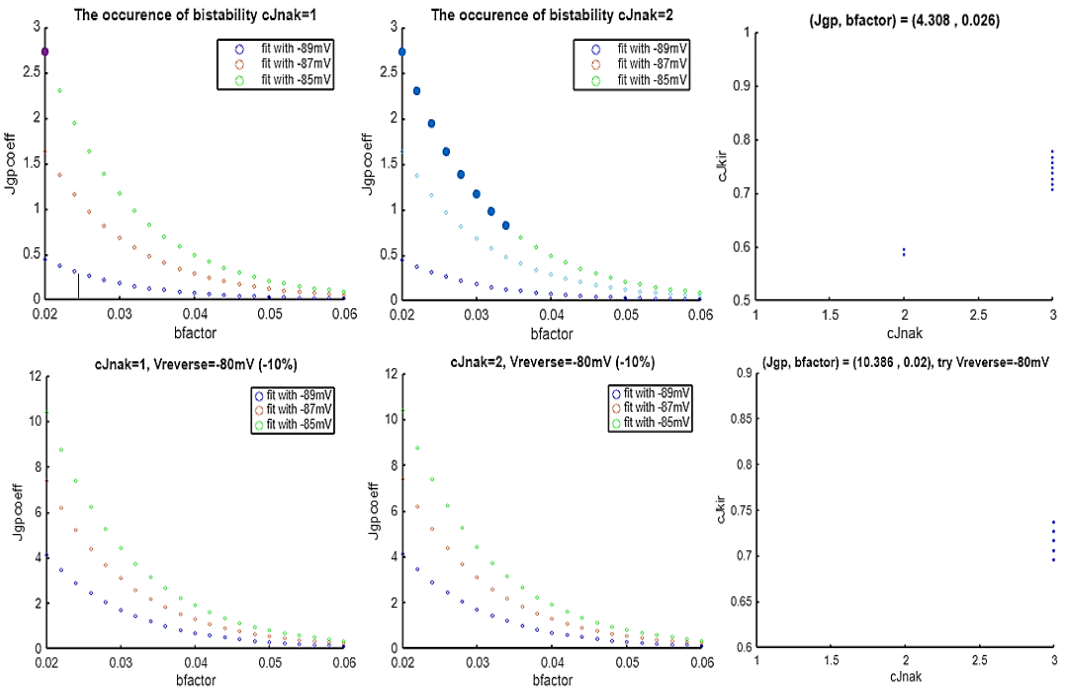

Fig 9. The possible parameter pairs corresponding with 3 resting membrane potential values at [K_{out}]= 4 mmol/L , the larger dots represent the existence of bistable solution(s) from at least 1 cJ_{kir} value ([0.1-1]) in both usual parameter fitting (upper row) and some modification at $V_{reverse}$ (lower row).

4. Discussion and conclusion

Both types of hypoPP are defined by the episodic paralytic condition with transcellular shift hypokalemia. Familial type is clearly suggested that it originates from the mutation of voltage sensor (either Nav or Cav) related to abnormal inward current whereas TPP which is a common subtype of nonfamilial type does not involve in aforementioned channels but is mainly driven by the activation of NaK+-ATPase from varying external factors [28]. Therefore, constructing the model with related components in TPP then extending to familial hypoPP is a good strategy. The developed model with the given re-identified

parameters yielded the results of changed membrane potential in both normal and pathologic experimental conditions which were consistent with experimental data in terms of qualitative characteristics. With the existence of bistability as mentioned in the experimental setup [12,19], this work tested by adding constraints corresponding with hypokalemia from transcellular shift without total depletion which is the real assumption in clinical practice and it also showed the occurrence of bistability in some parameter pairs (c_{Jnak} , c_{Jkir}). They also demonstrated the falling of extracellular potassium trajectories after supplementation from moving to one another stable point that could be the alternative way of exploitation of bifurcation in the nonlinear dynamical system instead of creating an addition term or equation and increasing the workload of parameter identification. The problem of sudden potassium falling could be fixed by calculating the mean of 2 trajectories from 2 initial points but the falling from 1 starting initial point could be fixed by searching the other parameter pair which yielded the monotonic trajectory as described in the proposed parameter mapping method. It is more suitable than conventional fitting method because it can ensure the nearby parameter values that yield the targeted qualitative phenomenon. The proportion of bistable solutions and the falling trajectories that increased with increasing coefficient of NaK+-ATPase current as the activation observed from parameter mapping of bistable solutions and the falling trajectories could support the hypothesis of the paradoxical hypokalemia in the case reports that came from higher NaK+-ATPase activation [29]. Moreover, some comparative study showed that patients who developed the paradoxical hypokalemia during treatment had significantly higher level of thyroxine, heart rate and systolic blood pressure linked to higher level of NaK+-ATPase activation [6]. Some experiment demonstrated that adding beta blocker which counteracted with beta-adrenergic stimulation at NaK+-ATPase during potassium treatment in hypokalemic phase of TPP could obviously increase the potassium level from the slow progressive phase [30]. In different structural model (familial hypoPP), after identifying suitable parameters, it also showed the increased possibility of bistable solution with increasing coefficient of NaK+-ATPase current as the same pattern in the TPP case. Therefore, NaK+-ATPase has the crucial role for potassium shift in nonlinear characteristics that need more quantitative experimental study to elucidate the interplay with other channels with abnormality. In terms of limitations, This model could not simulate the hyperpolarization after insulin infusion because it needed Na+ component which was out of the scope to be calculated. Moreover, to make the trajectory fit to the real data, additional term in equations is still required. The method of reduction of sharpness of falling mainly aims to keep the crucial feature realistically.

Challenges and the future work : How to improve the computational speed and to be more generalized when using the parameter mapping method? , What if this structure is connected to other sub-system in the body? Is it possible to extend this structural model to the total potassium depletion case?

This study was supported by Biomedical Engineering Institute, Chiang Mai University through the graduate scholarship.

References

1. McDonough, A. A., & Fenton, R. A. (2022). Potassium homeostasis: sensors, mediators, and targets. Pflugers Archiv : European journal of physiology, **474(8),** 853–867. https://doi.org/10.1007/s00424-022-02718-3
2. Weiss, J. N., Qu, Z., & Shivkumar, K. (2017). Electrophysiology of Hypokalemia and Hyperkalemia. Circulation. Arrhythmia and electrophysiology, **10(3)**, e004667. https://doi.org/10.1161/CIRCEP.116.004667

3. Kardalas, E., Paschou, S. A., Anagnostis, P., Muscogiuri, G., Siasos, G., & Vryonidou, A. (2018). Hypokalemia: a clinical update. Endocrine connections, **7(4)**, R135–R146. https://doi.org/10.1530/EC-18-0109
4. Statland, J. M., Fontaine, B., Hanna, M. G., Johnson, N. E., Kissel, J. T., Sansone, V. A., Shieh, P. B., Tawil, R. N., Trivedi, J., Cannon, S. C., & Griggs, R. C. (2018). Review of the Diagnosis and Treatment of Periodic Paralysis. Muscle & nerve, **57(4)**, 522–530. https://doi.org/10.1002/mus.26009
5. Antonello, I. C., Antonello, V. S., de Los Santos, C. A., de Almeida, N., & d'Avila, D. O. (2009). Thyrotoxic hypokalemic periodic paralysis: a life-threatening syndrome. European journal of emergency medicine : official journal of the European Society for Emergency Medicine, **16(1)**, 43–44. https://doi.org/10.1097/MEJ.0b013e328302622d
6. Shiang, J. C., Cheng, C. J., Tsai, M. K., Hung, Y. J., Hsu, Y. J., Yang, S. S., Chu, S. J., & Lin, S. H. (2009). Therapeutic analysis in Chinese patients with thyrotoxic periodic paralysis over 6 years. European journal of endocrinology, **161(6)**, 911–916. https://doi.org/10.1530/EJE-09-0553
7. Ryan, D. P., da Silva, M. R., Soong, T. W., Fontaine, B., Donaldson, M. R., Kung, A. W., Jongjaroenprasert, W., Liang, M. C., Khoo, D. H., Cheah, J. S., Ho, S. C., Bernstein, H. S., Maciel, R. M., Brown, R. H., Jr, & Ptácek, L. J. (2010). Mutations in potassium channel Kir2.6 cause susceptibility to thyrotoxic hypokalemic periodic paralysis. Cell, **140(1)**, 88–98. https://doi.org/10.1016/j.cell.2009.12.024
8. Zhang, Z., & Xiao, B. (2023). Case report: SCN4A p.R1135H gene variant in combination with thyrotoxicosis causing hypokalemic periodic paralysis. Frontiers in neurology, **13**, 1078784. https://doi.org/10.3389/fneur.2022.1078784
9. Francis, D. G., Rybalchenko, V., Struyk, A., & Cannon, S. C. (2011). Leaky sodium channels from voltage sensor mutations in periodic paralysis, but not paramyotonia. Neurology, **76(19)**, 1635–1641. https://doi.org/10.1212/WNL.0b013e318219fb57
10. Stadt MM, Leete J, Devinyak S, Layton AT (2022) A mathematical model of potassium homeostasis: Effect of feedforward and feedback controls. PLOS Computational Biology **18(12)**: e1010607. https://doi.org/10.1371/journal.pcbi.1010607
11. Ursino, M., & Donati, G. (2017). Mathematical Model of Potassium Profiling in Chronic Dialysis. Contributions to nephrology, **190**, 134–145. https://doi.org/10.1159/000468960
12. van Mil, H., Siegenbeek van Heukelom, J., & Bier, M. (2003). A bistable membrane potential at low extracellular potassium concentration. Biophysical chemistry, **106(1)**, 15–21. https://doi.org/10.1016/s0301-4622(03)00135-2
13. Delmoe, M., & Secomb, T. W. (2023). Conditions for Kir-induced bistability of membrane potential in capillary endothelial cells. Mathematical biosciences, **355**, 108955. https://doi.org/10.1016/j.mbs.2022.108955
14. Cheng, C. J., Kuo, E., & Huang, C. L. (2013). Extracellular potassium homeostasis: insights from hypokalemic periodic paralysis. Seminars in nephrology, **33(3)**, 237–247. https://doi.org/10.1016/j.semnephrol.2013.04.004
15. Puwanant, A., & Ruff, R. L. (2010). INa and IKir are reduced in Type 1 hypokalemic and thyrotoxic periodic paralysis. Muscle & nerve, **42(3)**, 315–327. https://doi.org/10.1002/mus.21693
16. Struyk, A. F., & Cannon, S. C. (2008). Paradoxical depolarization of BA2+- treated muscle exposed to low extracellular K+: Insights into resting potential abnormalities in hypokalemic paralysis. Muscle & Nerve, **37(3)**, 326-337. https://doi.org/10.1002/mus.20928
17. Yang Y, Chen F, Karasawa T, Ma KT, Guan BC, et al. (2015) Diverse Kir Expression Contributes to Distinct Bimodal Distribution of Resting Potentials and Vasotone

Responses of Arterioles. PLOS ONE **10(5)**: e0125266. https://doi.org/10.1371/journal.pone.0125266
18. Zacchia, M., Abategiovanni, M. L., Stratigis, S., & Capasso, G. (2016). Potassium: From Physiology to Clinical Implications. Kidney diseases (Basel, Switzerland), **2(2)**, 72–79. https://doi.org/10.1159/000446268
19. Jurkat-Rott, K., Weber, M. A., Fauler, M., Guo, X. H., Holzherr, B. D., Paczulla, A., Nordsborg, N., Joechle, W., & Lehmann-Horn, F. (2009). K+-dependent paradoxical membrane depolarization and Na+ overload, major and reversible contributors to weakness by ion channel leaks. Proceedings of the National Academy of Sciences of the United States of America, **106(10)**, 4036–4041. https://doi.org/10.1073/pnas.0811277106
20. Allon, M. (2013). Disorders of Potassium Metabolism. National Kidney Foundation Primer on Kidney Diseases (Sixth Edition), 90-99. https://doi.org/10.1016/B978-1-4557-4617-0.00010-8
21. Seifter, J. L. (2011). Potassium Disorders. Goldman's Cecil Medicine (Twenty-Fourth Edition), 734-741. https://doi.org/10.1016/B978-1-4377-1604-7.00119-6
22. Dhamoon, A. S., & Jalife, J. (2005). The inward rectifier current (IK1) controls cardiac excitability and is involved in arrhythmogenesis. Heart Rhythm, **2(3)**, 316-324. https://doi.org/10.1016/j.hrthm.2004.11.012
23. Ruff R. L. (1999). Insulin acts in hypokalemic periodic paralysis by reducing inward rectifier K+ current. Neurology, **53(7)**, 1556–1563. https://doi.org/10.1212/wnl.53.7.1556
24. Quayle, J. M., Dart, C., & Standen, N. B. (1996). The properties and distribution of inward rectifier potassium currents in pig coronary arterial smooth muscle. The Journal of physiology, **494(3)**, 715–726. https://doi.org/10.1113/jphysiol.1996.sp021527
25. Lin, S. H., & Lin, Y. F. (2001). Propranolol rapidly reverses paralysis, hypokalemia, and hypophosphatemia in thyrotoxic periodic paralysis. American journal of kidney diseases : the official journal of the National Kidney Foundation, **37(3)**, 620–623.
26. Chandramohan, G., Dineshkumar, T., Arul, R., Seenivasan, M., Dhanapriya, J., Sakthirajan, R., Balasubramaniyan, T., & Gopalakrishnan, N. (2018). Spectrum of Hypokalemic Paralysis from a Tertiary Care Center in India. Indian journal of nephrology, **28(5)**, 365–369. https://doi.org/10.4103/ijn.IJN_225_17
27. Struyk, A. F., & Cannon, S. C. (2007). A Na+ channel mutation linked to hypokalemic periodic paralysis exposes a proton-selective gating pore. The Journal of general physiology, **130(1)**, 11–20. https://doi.org/10.1085/jgp.200709755
28. Lin, S. H., & Huang, C. L. (2012). Mechanism of thyrotoxic periodic paralysis. Journal of the American Society of Nephrology : JASN, **23(6)**, 985–988. https://doi.org/10.1681/ASN.2012010046
29. Bilha, S., Mitu, O., Teodoriu, L., Haba, C., & Preda, C. (2020). Thyrotoxic Periodic Paralysis-A Misleading Challenge in the Emergency Department. Diagnostics (Basel, Switzerland), **10(5)**, 316. https://doi.org/10.3390/diagnostics10050316
30. Tse Tan, S. Y., Xiong, J., Puar, T. H., Khoo, J., & Soh, S. B. (2021). Acute Flaccid Tetraparesis after COVID-19 Infection: Think of the Thyroid. Case Reports in Medicine, 2022(1), 5827664. https://doi.org/10.1155/2022/5827664